

# Simulation of laser beam transformation in a dual feedback nonlinear ring interferometer

I.V. Izmailov,<sup>1</sup> A.V. Lyachin,<sup>1</sup> A.L. Magazinnikov,<sup>2</sup>  
B.N. Poizner,<sup>1</sup> and D.A. Shergin<sup>1</sup>

<sup>1</sup>Tomsk State University,

<sup>2</sup>Tomsk State University of Control Systems and Radioelectronics

Received October 14, 2005

We propose to supplement the nonlinear ring interferometer (NRI) with two-dimensional feedback, known since 1979, with second feedback loop (FBL) arranged by adding two mirrors. To study the regular and random modes of operation of a dual feedback NRI (DNRI), we have constructed the mathematical model that allows for multiple passes and the model based on loss approximation. The computational algorithms have been constructed and the bifurcation behavior of the DNRI has been analyzed. The data obtained allow determining the sets of DNRI physical parameters that govern the transition from the static mode of operation to the dynamic one (including the deterministic chaos). It is supposed that owing to various turns and time lags of a laser beam in two FBLs (when either various systems of coupled oscillators or the system of additional coupling in an oscillator are formed in the DNRI) such an interferometer has advantages as a coder in a system of confidential communication lines.

The experiments have shown that nonlinear ring interferometer (NRI) is represented as an example of optical system capable of generating both regular optical structures and the deterministic chaos.<sup>1-4</sup>

Since the middle of 1990s, the development of principles and data-processing units using NRI as well as its fiber-optic analogs, made up an independent branch in the information optics.<sup>1,5</sup> Specifically, the deterministic chaos condition is thoroughly investigated within the frameworks of the developments of systems for confidential communication. We have analyzed the optical, physical, and nonlinear dynamical phenomena in this NRI and in the cryptosystem based on it.<sup>6,7</sup>

To increase the cryptostability of the confidential communication and to widen the possibilities of controlling the number, type, and mutual bracing (constellation) of static conditions in a phase space of the dynamic system, it is proposed to supplement the NRI optical layout with a second feedback loop (FBL). The large scale transformation of light field (of the FBL<sub>1</sub>-type or another), losses, field time lag, and phase shift can take place in the FBL<sub>2</sub>. The assumption that the control over parameters of laser radiation can be improved well agrees with the conclusions drawn in Ref. 8 that the use of a spatial Fourier filter in additional FBL allows one to affect the formation of structures and suppress the turbulent regime.

In order to check the assumptions made, it is necessary to construct a mathematical model of the processes in the DNRI, to find its stationary solutions, and to analyze their stability. It is also necessary to find out the features of bifurcation behavior using a model of the DNRI, as well to look for possibilities of controlling this behavior and possible advantages of DNRI over the NRI in terms of stability to attempts of "cracking" the cryptosystem.

## Description of scheme and model of a dual feedback NRI

The optical arrangements of the NRI and DNRI are presented in Fig. 1. Here  $E_{\text{inp}}$  and  $E_{\text{outp}}$  are the input and output fields of the NRI, NM is the nonlinear medium (for instance, liquid crystal) of the length  $l$ ,  $G$  and  $G_i$  are the linear elements that perform the large scale transformations of the optical field (turn by the angle  $\Delta$  and  $\Delta_i$ , shift, compression or extension in the plane  $xOy$  of the laser beam cross section),  $M_i$  are the mirrors.

A model describing the dynamics of nonlinear phase shift  $U$  in a DNRI, with a bichromatic optical field, whose projections  $E_x(\mathbf{r}, t)$ ,  $E_y(\mathbf{r}, t)$  are

$$\begin{aligned} E_x(\mathbf{r}, t) &= a(\mathbf{r}, t) \cos[(\omega + \Omega)t + \Psi(\mathbf{r}, t)] + \\ &+ b(\mathbf{r}, t) \cos[(\omega - \Omega)t + \Theta(\mathbf{r}, t)], \\ E_y(\mathbf{r}, t) &= a(\mathbf{r}, t) \sin[(\omega + \Omega)t + \Psi(\mathbf{r}, t)] - \\ &- b(\mathbf{r}, t) \sin[(\omega - \Omega)t + \Theta(\mathbf{r}, t)], \end{aligned}$$

has the form of a partial differential equation with the right-hand side containing the function  $f(\mathbf{r}, t)$  that nonlinearly depends on  $U(\mathbf{r}, t)$ :

$$\tau_n(\mathbf{r}) \partial U(\mathbf{r}, t) / \partial t = D_e(\mathbf{r}) \Delta U(\mathbf{r}, t) - U(\mathbf{r}, t) + f(\mathbf{r}, t); \quad (1)$$

$$f(\mathbf{r}, t) = Q_a K n_{2n}(\mathbf{r}) a_n^2(\mathbf{r}, t) + K(1 - Q_a) n_{2n}(\mathbf{r}) b_n^2(\mathbf{r}, t);$$

$$a_n(\mathbf{r}, t) = (Ac_a^2 + As_a^2)^{0.5}; \quad b_n(\mathbf{r}, t) = (Ac_b^2 + As_b^2)^{0.5};$$

$$\Psi(\mathbf{r}, t) = \text{Arg}(Ac_a, As_a); \quad \Theta(\mathbf{r}, t) = \text{Arg}(Ac_b, As_b);$$

$$\begin{aligned} Ac_a &= a_{\text{inp}n}(\mathbf{r}, t) \cos[\Psi_{\text{inp}}(\mathbf{r}, t)] + 0.5\gamma_1(\mathbf{r}'_1, t) \times \\ &\times a_n(\mathbf{r}'_1, t - \tau_1) \cos[\Psi(\mathbf{r}'_1, t - \tau_1) - (1 + q)\omega\tau_1] / \sigma_1 + \\ &+ 0.5\gamma_2(\mathbf{r}'_2, t) a_n(\mathbf{r}'_2, t - \tau_2) \cos[\Psi(\mathbf{r}'_2, t - \tau_2) - (1 + q)\omega\tau_2] / \sigma_2, \end{aligned}$$

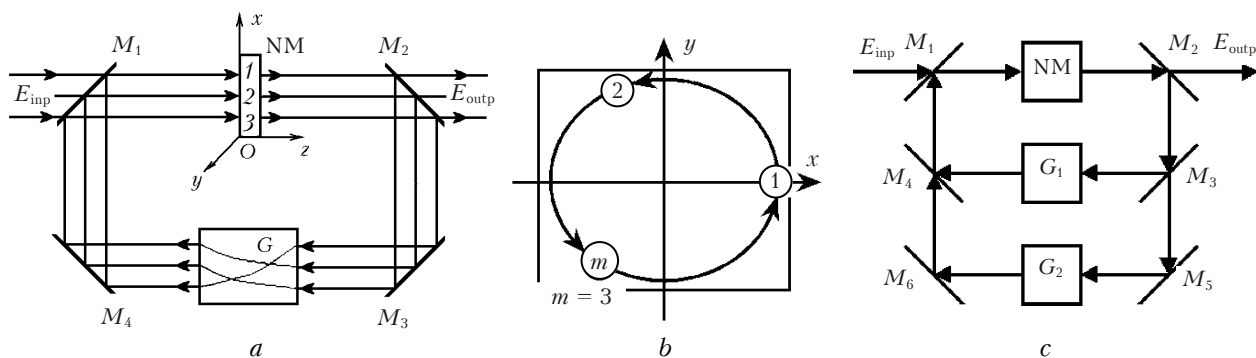


**Fig. 1.** Optical trains of NRI (a) and double-circuit NRI (c). NRI and ray path in NRI when turning the light field (by  $G$ -element) at  $\Delta = 360^\circ/m = 120^\circ$  in the plane  $xOy$ : the ray paths 1, 2, 3, closed after three tracings (a); the ray path projection 1, 2, 3 to the plane  $xOy$  (b).

$$\begin{aligned}
 A_{S_a} &= a_{\text{inp}n}(\mathbf{r}, t) \sin[\Psi_{\text{inp}}(\mathbf{r}, t)] + 0.5\gamma_1(\mathbf{r}'_1, t) \times \\
 &\times a_n(\mathbf{r}'_1, t - \tau_1) \sin[\Psi(\mathbf{r}'_1, t - \tau_1) - (1 + q)\omega\tau_1/\sigma_1 + \\
 &+ 0.5\gamma_2(\mathbf{r}'_2, t) a_n(\mathbf{r}'_2, t - \tau_2) \cos[\Psi(\mathbf{r}'_2, t - \tau_2) - (1 + q)\omega\tau_2/\sigma_2, \\
 A_{C_b} &= b_{\text{inp}n}(\mathbf{r}, t) \cos[\Theta_{\text{inp}}(\mathbf{r}, t)] + 0.5\gamma_1(\mathbf{r}'_1, t) \times \\
 &\times b_n(\mathbf{r}'_1, t - \tau_1) \cos[\Theta(\mathbf{r}'_1, t - \tau_1) - (1 - q)\omega\tau_1/\sigma_1 + \\
 &+ 0.5\gamma_2(\mathbf{r}'_2, t) b_n(\mathbf{r}'_2, t - \tau_2) \cos[\Theta(\mathbf{r}'_2, t - \tau_2) - (1 - q)\omega\tau_2/\sigma_2, \\
 A_{S_b} &= b_{\text{inp}n}(\mathbf{r}, t) \sin[\Theta_{\text{inp}}(\mathbf{r}, t)] + 0.5\gamma_1(\mathbf{r}'_1, t) \times \\
 &\times b_n(\mathbf{r}'_1, t - \tau_1) \sin[\Theta(\mathbf{r}'_1, t - \tau_1) - (1 - q)\omega\tau_1/\sigma_1 + \\
 &+ 0.5\gamma_2(\mathbf{r}'_2, t) b_n(\mathbf{r}'_2, t - \tau_2) \sin[\Theta(\mathbf{r}'_2, t - \tau_2) - (1 - q)\omega\tau_2/\sigma_2.
 \end{aligned}$$

Here  $\mathbf{r} \equiv (x, y)$  is the radius-vector of the cross section  $xOy$ ;  $\tau_n$  is the relaxation time of a nonlinear part of the refractive index of an  $l$ -long NM,  $D_e$  is the normalized coefficient of molecular diffusion in NM.  $\Psi$ ,  $\Theta$  and  $\Psi_{\text{inp}}$ ,  $\Theta_{\text{inp}}$  are the input field phases of NM and NRI;

$$\begin{aligned}
 a_n(\mathbf{r}, t) &= a(\mathbf{r}, t) / [(1 - R_1)^{0.5} a_{\text{inp max}\{r,t\}}], \\
 b_n(\mathbf{r}, t) &= b(\mathbf{r}, t) / [(1 - R_1)^{0.5} b_{\text{inp max}\{r,t\}}]; \\
 a_{\text{inp}n}(\mathbf{r}, t) &= a_{\text{inp}}(\mathbf{r}, t) / a_{\text{inp max}\{r,t\}}; \\
 b_{\text{inp}n}(\mathbf{r}, t) &= b_{\text{inp}}(\mathbf{r}, t) / b_{\text{inp max}\{r,t\}}
 \end{aligned}$$

are the normalized field amplitudes at input of NM and NRI;  $a_{\text{inp max}\{r,t\}}$ ,  $b_{\text{inp max}\{r,t\}}$  are the maximum values of the input field amplitudes,

$$\tau_i \equiv \tau_i(\mathbf{r}'_i, t) = t_{ei}(\mathbf{r}'_i, t) + U[\mathbf{r}'_i, t - t_{ei}(\mathbf{r}'_i, t)]/\omega$$

is the propagation time of the light field component passing (through the  $i$ th FBL) by the time moment  $t$  to the point  $\mathbf{r}$  of the NM input plane from the point  $\mathbf{r}'_i$  of the same plane (total lag time, time of the complete roundtrip in the interferometer through the  $i$ th FBL);  $t_{ei}$  is the equivalent lag time in the  $i$ th FBL of the DNRI;

$$\begin{aligned}
 q &\equiv \Omega/\omega; Q_a = K_a/K; K = K_a + K_b, \\
 K_a &= (1 - R_1) a_{oe} n_{2 \text{ max}\{r\}} l k (a_{\text{inp max}\{r,t\}})^2, \\
 K_b &= (1 - R_1) a_{oe} n_{2 \text{ max}\{r\}} l k (b_{\text{inp max}\{r,t\}})^2
 \end{aligned}$$

are the parameters determining the force due to nonlinear effects;

$$n_{2n}(\mathbf{r}) = n_2(\mathbf{r})/n_{2 \text{ max}\{r\}}$$

is the normalized parameter of nonlinear refraction,  $n_{2 \text{ max}\{r\}}$  is the maximum value of the nonlinear refraction parameter,  $k = |\mathbf{k}| = \omega/c$  is the wave number;

$$\begin{aligned}
 \gamma_1(\mathbf{r}'_1, t) &\equiv 2C_n(\mathbf{r}'_1) \kappa_1(\mathbf{r}'_1, t) R_I, \\
 \gamma_2(\mathbf{r}'_2, t) &\equiv 2C_n(\mathbf{r}'_2) \kappa_2(\mathbf{r}'_2, t) R_{II}
 \end{aligned}$$

are the doubled amplitude transmission coefficients (doubled coefficients of loss /transmission) in the FBL<sub>1</sub> and FBL<sub>2</sub>,  $C_n$ ,  $\kappa_1$ ,  $\kappa_2$  are the losses in NM and FBL elements of DNRI;

$$R_I \equiv (R_2 R_3 R_4 R_1)^{1/2};$$

$$R_{II} \equiv [R_2 (1 - R_3) (1 - R_4) R_1]^{1/2};$$

$R_i$  are the refraction coefficients of the corresponding mirrors;  $\sigma_i$  is the coefficient of beam extension in the  $i$ th FBL.

Let us operate, in what follows, with the model in the so-called *point approximation* (point model) that follows from the above stated, if one assumes that no molecular diffusion of NM exists, i.e.,  $D_e = 0$ . By turning at an angle  $\Delta_j = 2\pi M_j/m$  (or shifting by  $\delta_j = M_j\delta$  times, or compressing by  $\sigma_j = M_j\sigma$  times), the model takes the form of a differential equation

$$\begin{aligned}
 \tau_{ni} dU_i(t)/dt &= -U_i(t) + Q_a K n_{2ni} a_{ni}^2(t) + \\
 &+ K(1 - Q_a) n_{2ni} b_{ni}^2(t); \quad (2) \\
 a_{ni}(t) &= (Ac_{ai}^2 + As_{ai}^2)^{0.5}; b_{ni}(t) = (Ac_{bi}^2 + As_{bi}^2)^{0.5}; \\
 \Psi_i(t) &= \text{Arg}(Ac_{ai}, As_{ai}); \Theta_i(t) = \text{Arg}(Ac_{bi}, As_{bi}); \\
 Ac_{ai} &= a_{\text{inp}ni}(t) \cos[\Psi_{\text{inp}i}(t)] + \\
 &+ 0.5\gamma_{1i-M_1}(t) a_{ni-M_1}(t - \tau_1) \times \\
 &\times \cos[\Psi_{i-M_1}(t - \tau_1) - (1 + q)\omega\tau_1/\sigma_1 + \\
 &+ 0.5\gamma_{2i-M_2}(t) a_{ni-M_2}(t - \tau_2) \times \\
 &\times \cos[\Psi_{i-M_2}(t - \tau_2) - (1 + q)\omega\tau_2/\sigma_2, \\
 As_{ai} &= a_{\text{inp}ni}(t) \sin[\Psi_{\text{inp}i}(t)] + 0.5\gamma_{1i-M_1}(t) \times \\
 &\times a_{ni-M_1}(t - \tau_1) \sin[\Psi_{i-M_1}(t - \tau_1) - (1 + q)\omega\tau_1/\sigma_1 +
 \end{aligned}$$

$$\begin{aligned}
& + 0.5\gamma_{2i-M_2}(t)a_{ni-M_2}(t-\tau_2) \times \\
& \times \sin[\Psi_{i-M_2}(t-\tau_2) - (1+q)\omega\tau_2]/\sigma_2, \\
Ac_{bi} &= b_{\text{inp}ni}(t)\cos[\Theta_{\text{inp}i}(t)] + 0.5\gamma_{1i-M_1}(t)b_{ni-M_1}(t-\tau_1) \times \\
& \times \cos[\Theta_{i-M_1}(t-\tau_1) - (1-q)\omega\tau_1]/\sigma_1 + \\
& + 0.5\gamma_{2i-M_2}(t)b_{ni-M_2}(t-\tau_2) \times \\
& \times \cos[\Theta_{i-M_2}(t-\tau_2) - (1-q)\omega\tau_2]/\sigma_2, \\
As_{bi} &= b_{\text{inp}ni}(t)\sin[\Theta_{\text{inp}i}(t)] + 0.5\gamma_{1i-M_1}(t)b_{ni-M_1}(t-\tau_1) \times \\
& \times \sin[\Theta_{i-M_1}(t-\tau_1) - (1-q)\omega\tau_1]/\sigma_1 + \\
& + 0.5\gamma_{2i-M_2}(t)b_{ni-M_2}(t-\tau_2) \times \\
& \times \sin[\Theta_{i-M_2}(t-\tau_2) - (1-q)\omega\tau_2]/\sigma_2,
\end{aligned}$$

where

$$\begin{aligned}
\tau_1 &\equiv \tau_{1i-M_1}(t) = t_{e1i-M_1}(t) + U_{i-M_1}[t - t_{e1i-M_1}(t)]/\omega, \\
\tau_2 &\equiv \tau_{2i-M_2}(t) = t_{e2i-M_2}(t) + U_{i-M_2}[t - t_{e2i-M_2}(t)]/\omega.
\end{aligned}$$

For the NRI operated in the static mode ( $d/dt = 0$ ), one can obtain the following relations:

$$\begin{aligned}
a_{ni} &= (Ac_{ai}^2 + As_{ai}^2)^{0.5}, \Psi_i = \text{Arg}(Ac_{ai}, As_{ai}); \\
b_{ni} &= (Ac_{bi}^2 + As_{bi}^2)^{0.5}, \Theta_i = \text{Arg}(Ac_{bi}, As_{bi}); \\
Ac_{ai} &= a_{\text{inp}ni}\cos[\Psi_{\text{inp}i}] + 0.5\gamma_{1i-M_1}a_{ni-M_1} \times \\
& \times \cos[\Psi_{i-M_1} - (1+q)\omega\tau_1]/\sigma_1 + \\
& + 0.5\gamma_{2i-M_2}a_{ni-M_2}\cos[\Psi_{i-M_2} - (1+q)\omega\tau_2]/\sigma_2, \\
As_{ai} &= a_{\text{inp}ni}\sin[\Psi_{\text{inp}i}] + 0.5\gamma_{1i-M_1}a_{ni-M_1} \times \\
& \times \sin[\Psi_{i-M_1} - (1+q)\omega\tau_1]/\sigma_1 + \\
& + 0.5\gamma_{2i-M_2}a_{ni-M_2}\sin[\Psi_{i-M_2} - (1+q)\omega\tau_2]/\sigma_2, \\
Ac_{bi} &= b_{\text{inp}ni}\cos[\Theta_{\text{inp}i}] + 0.5\gamma_{1i-M_1}b_{ni-M_1} \times \\
& \times \cos[\Theta_{i-M_1} - (1-q)\omega\tau_1]/\sigma_1 + \\
& + 0.5\gamma_{2i-M_2}b_{ni-M_2}\cos[\Theta_{i-M_2} - (1-q)\omega\tau_2]/\sigma_2, \\
As_{bi} &= b_{\text{inp}ni}\sin[\Theta_{\text{inp}i}] + 0.5\gamma_{1i-M_1}b_{ni-M_1} \times \\
& \times \sin[\Theta_{i-M_1} - (1-q)\omega\tau_1]/\sigma_1 + \\
& + 0.5\gamma_{2i-M_2}b_{ni-M_2}\sin[\Theta_{i-M_2} - (1-q)\omega\tau_2]/\sigma_2; \\
\tau_1 &\equiv \tau_{1i-M_1} = t_{e1i-M_1} + U_{i-M_1}/\omega, \\
\tau_2 &\equiv \tau_{2i-M_2} = t_{e2i-M_2} + U_{i-M_2}/\omega; \\
U_i &= Q_a K n_{2ni} a_{ni}^2 + K(1 - Q_a) n_{2ni} b_{ni}^2, \quad (3)
\end{aligned}$$

where  $i$  is the order number of a point in the chain of transposition points (in the laser beam cross section). It is obvious that the obtained expression (2) can be interpreted as a vector function of the vector argument  $\mathbf{E}_i = \mathbf{F}(\mathbf{E}_{i-M_1}, \mathbf{E}_{i-M_2})$ , where  $\mathbf{E}_i \equiv (a_{ni}, \Psi_i, b_{ni}, \Theta_i)$  is used.

Let  $M_1 \geq M_2$ . Then, a model of *space* changes in amplitudes  $a_{ni}$ ,  $b_{ni}$  and phases  $\Psi_i$ ,  $\Theta_i$  of the fields in DNRI is represented by means of *discrete mapping* (DM), which consists of the  $M_1$  vector equations determined through the function  $\mathbf{E}_i$ . Moreover, DM has dimensionality of  $4M_1$ :

$$\begin{aligned}
\mathbf{E}_{i+1,l} &= \mathbf{F}\{\mathbf{E}_{i,l-0M_2}, \mathbf{F}\{\mathbf{E}_{i,l-1M_2}, \mathbf{F}\{\mathbf{E}_{i,l-2M_2}, \dots \\
& \dots, \mathbf{F}\{\mathbf{E}_{i,l-nM_2}, \mathbf{E}_{i,M_1-M_2+j}\}\}\}, \quad (4)
\end{aligned}$$

where the subscript  $i$  denotes the discrete *evolutionary variable* (corresponding to a group of points from the chain of transposition points), i.e., it is an analog of time,  $l = nM_2 + j$ ,  $l, n, j$  are the integers, such that  $l = [1; M_1]$ ;  $j = [1; M_2 - 1]$ .

The presence of two FBLs gives rise to the variety of combinations for space field transformations in each of the FBLs.

### Chain of transposition points and specific features of DNRI interpretation as a system of coupled oscillators

Spatial transformation of light field conducted by means of linear elements  $G_i$ , causes the type of chain of transposition points (CTP). For elementary field transformations in a  $G$ -element of a single feedback NRI, the CTP-types are shown in Table 1. In its turn, the type of CTP determines the structure of mutual dependence for the values of dynamic variables, i.e., the dependence of  $U_{i+1}$  on  $U_i$ , in conjunction with characteristics of (un)closeness and (in)finity finitude.

As to DNRI, complication of the CTP-structure can take place both due to the inevitable expansion of typology, and because of the complication inside each of the above-mentioned CTP-type.

Assume that turn of light field takes place in the  $i$ th FBL by the angle  $\Delta_i = 2\pi M_i/m$ , where  $m$  is the number of points from the NRI considered, i.e., the *number of points* in the CTP. For instance, in Table 1 for the single feedback loop NRI, where  $\Delta = 120^\circ$ ,  $m = 3$ . The quantity  $2\pi/m$  is the "quantum" of the turn angle, i.e., the minimum-turn angle at the preset  $m$  value. Then,  $M_i$  is the numerical expression (in units of  $2\pi/m$ ) of the field turn angle  $\Delta_i$ , or, with regard for the CTP, the movement pitch size on CTP.

Therefore, according to combinations of the values  $M_i$  and  $m$ , the CTP-structure changes appreciably. Three numbers (subscripts) are  $m$ ,  $M_1$ ,  $M_2$  can be considered as a natural "coding" of the structure. This coding is used in Table 2 and further in the text, where different configurations of transitions between the points in CTP are presented. Figures in Table 2 denote transitions between the points in CTP by lines: dashed lines denote transitions in FBL<sub>1</sub>, solid lines denote transitions in FBL<sub>2</sub>. Table 2 shows how diversely the CTP-structure becomes complicated with the growth of  $m$  due to the presence of the second feedback, FBL<sub>2</sub>. In case of one FBL, Table 2 would contain only one cell corresponding to the triad  $m11$ . However, the way of representing, used in Table 1, is too redundant. For instance, the CTP  $mmm$  is decomposed into  $m$  CTP 111.

**Table 1. Connection between the elementary transformations of a laser beam in FBL of NRI (setting the chain configuration of transposition points) and the optical structure  $U(r, t)$ , being formed in the beam cross section**

Elementary types of beam transformation by the $G$ -element			
Turn ( $\Delta = 2\pi M/m$ )	Shift ( $\delta$ )	Compression ( $1/\sigma$ )	Extension ( $\sigma$ )
CTP-type			
Closed finite	Unclosed finite	Unclosed infinite	
		$(m = \infty)$	$(m = -\infty)$
The idealized structures formed			

**Table 2. Configuration of transitions between the points in CTP in case of “three-point” ( $m = 3$ ) model of processes in DNRI**

$m = 3$		$M_2$		
		1	2	3
$M_1$	1			
	2			
	3			

If  $m$  is a prime number, only the first line is urgent in such Tables, all the rest configurations of transitions can be expressed through the configurations existing in it. Otherwise, one should choose the values of triple subscripts in tables according to the following rule:  $m = M_1 N_1$ ,  $m = M_2 N_2$ , where  $M_1$  and  $M_2$  are the mutually prime numbers. For instance, for a CTP consisted of six points,  $M_1 = 3$  is realized for  $N_1 = 2$  (two-point structures) and  $M_2 = 2$  for  $N_2 = 3$  (three-point structures).

The case of 313 can be interpreted in Table 2 as a system of *three* coupled oscillators, i.e., single

feedback “single-point” NRI. This connection is provided by the second feedback: laser beam energy of one of the above-mentioned NRI goes into another NRI through this feedback successively and effects the dynamics (mode type), and, probably, the synchronization of oscillations in them. The parameter  $\gamma_2$  serves a coupling coefficient between the NRIs.

On the contrary, the case of CTP 311 and 312, apparently, should be interpreted as emergence of a system of three additional couplings in one oscillator (“three-point” NRI) owing to the second FBL arranged. This property manifests itself in a more evident way at  $m = 5$  and higher.

## Simulation data

### Peculiarities in the structure of bifurcation diagrams

According to the statement of the problem, it is necessary to find the stationary solutions and to analyze their stability. It is expedient to simplify the task, having restricted oneself to the approximation of strong losses ( $R^2 C_n \ll 1$ , i.e., when the light field component after the second NM pass is considered negligible, and by assuming the absence of a time lag ( $t_{ej} \ll \tau_n$ ) for the single-frequency field ( $Q_a = 1$ ,  $b_{\text{inp}i}(t) = 0$ ,  $q = 0$ ) in the FBL. Therefore, assuming that  $\omega t_{ej} \approx 2\pi N$ , one has a simplified version, instead of the model (2):

$$\tau_{ni} dU_i(t)/dt = -U_i(t) + K[1 + \gamma_{12} \cos(U_{i-M_1}(t)) + \gamma_{13} \cos(U_{i-M_2}(t)) + \gamma_{23} \cos(U_{i-M_1}(t) - U_{i-M_2}(t))], \quad (5)$$

where  $\gamma_{ij}$  characterize the interference pattern visibility and are caused by radiation losses in the FBL:

$$\gamma_{12} = 2R_1 \kappa_1 C_n, \quad \gamma_{13} = 2R_{II} \kappa_2 C_n, \quad \gamma_{23} = 2R_{II} R_1 \kappa_1 \kappa_2 C_n.$$

Henceforth, it is necessary to compare the results obtained for the models of single and dual feedback loop interferometers. It is advisable to use for this purpose the factor of radiation loss / transmission (for the amplitude)  $\gamma = 2R\kappa C_n$  for one pass through the FBL of a single feedback loop NRI. One can show that  $\gamma_{12} = \gamma(R_3 R_4)^{1/2} \kappa_1 / \kappa$ ,  $\gamma_{13} = \gamma(1 - (R_3 R_4)^{1/2}) \kappa_2 / \kappa$ , and  $\gamma_{23} = \gamma^2 (R_3 R_4)^{1/2} (1 - (R_3 R_4)^{1/2}) \kappa_1 \kappa_2 / (2\kappa^2)$ . In dealing with the model (5), it is convenient to set values of  $\gamma$  at  $(R_3 R_4)^{1/2} = 0.5$  and  $\kappa_1 = \kappa_2$ , then  $\gamma_{12} = \gamma_{13}$ .

To analyze the model properties, the bifurcation diagrams are constructed (static ( $dU_i(t)/dt = 0$ ) here) for the dependence of solution on the selected bifurcation parameter. The field turn by the angles of 0 and 180, 0 and 120, 0 and 90, 90 and 180, 120 and 180° are considered. Figure 2 gives a general idea of the evolution of bifurcation diagrams (BD) for a single feedback loop interferometer (Fig. 1a) with the account of the field turn in the FBL.

For estimation of the additional effect of FBL on the BD structure, the simulation has been carried out, when the field turn is performed in only one loop. It is established that BDs are identical by structure for the model of a single feedback loop interferometer at field turn angles in the loop being  $\Delta_1 = 180^\circ$ ,  $\Delta_2 = 0^\circ$  or  $\Delta_1 = 90^\circ$ ,  $\Delta_2 = 0^\circ$  ignoring time lag and field turn in the FBL at the corresponding values of the radiation losses (Fig. 2a).

The form of BD for a "point" model of DNRI is analyzed in Fig. 2 at  $\gamma = 0.8$ ,  $(R_3 R_4)^{1/2} = 0.5$  and  $\Delta_1 = 180^\circ$ ,  $\Delta_2 = 0^\circ$ , or  $\Delta_1 = 120^\circ$ ,  $\Delta_2 = 0^\circ$ , or  $\Delta_1 = 90^\circ$ ,  $\Delta_2 = 0^\circ$  in the approximation of strong losses and neglecting the time lags  $t_{ei}$  for the field in FBLs with equal losses ( $\gamma_{12} = \gamma_{13} = 0.5\gamma$ ). It turns out that if an optical field in the laser beam cross section is turned

by  $\Delta_i = 2\pi M_i / m$  (where  $i = 1, 2$ ), and  $\Delta_i = 0$ ,  $\Delta_j \neq 0$ , then

- at *even*  $m$ , the BD structure is the same as for the single feedback model of the NRI with  $\Delta = 0$ ;
- at *odd*  $m$ , the BD structures for the model of DNRI are essentially different from those for the models of NRI both with  $\Delta = \Delta_i$  and with  $\Delta = \Delta_j$ .

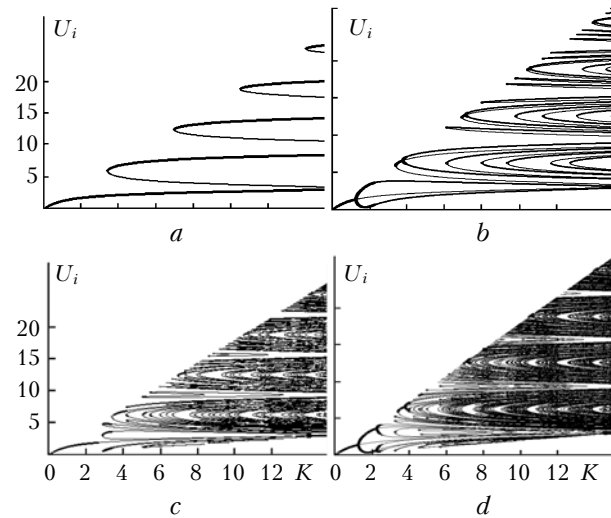


**Fig. 2.** Bifurcation diagrams (statistic solution on the plane  $U_i$  is the nonlinearity parameter  $K$  at  $\gamma = 0.8$ ) for a single feedback loop NRI at a field turn angles in the loop:  $\Delta = 0^\circ$  (a);  $180^\circ$  (b);  $120^\circ$  (c);  $90^\circ$  (d). Stationary sections of branches are denoted by bold lines.

Figure 3 presents the BD for the model of DNRI showing a series of characteristics.

1) No bistability occurs at  $K \in [2.0; 5.1]$ . This is caused by the contradiction in the bistability conditions for single feedback systems at  $\Delta = 180$  and  $90^\circ$ .

2) Configuration of stable and unstable BD branches changes significantly. Unlike the single feedback system with  $\Delta = 90^\circ$ , the stable regions appear at  $K > 8$ .

3) The position of BD branches corresponding to the equal values of the phase shifts  $U_i$ , remains constant. This fact follows directly from the model and serves a verification example.

In comparing Figs. 3c and d, one can state that the increase in  $m$  of the CTP points, which occurs at change of the field turn angle in one of FBLs, increase in the number of branches is observed at smaller values of nonlinearity coefficient  $K$ , i.e., at lower levels of input radiation.

As follows from analysis of a number of (un)stable BD branches, the second FBL serves the DNRI control means as a generator of the deterministic chaos. Structure of the BD for the model of DNRI at  $\Delta_1 = 90^\circ$ ,  $\Delta_2 = 180^\circ$  at different ratios of loss / transmission coefficients  $\gamma_{12}/\gamma_{13}$  (due to the difference of  $(R_3 R_4)^{1/2}$  from 0.5 or change in  $\kappa_i$ ), when  $\gamma = 0.5$ , have shown that BD structure essentially depends not only on ratio  $\gamma_{12}/\gamma_{13}$ , but also on the values  $\gamma_{12}$  and  $\gamma_{13}$ .

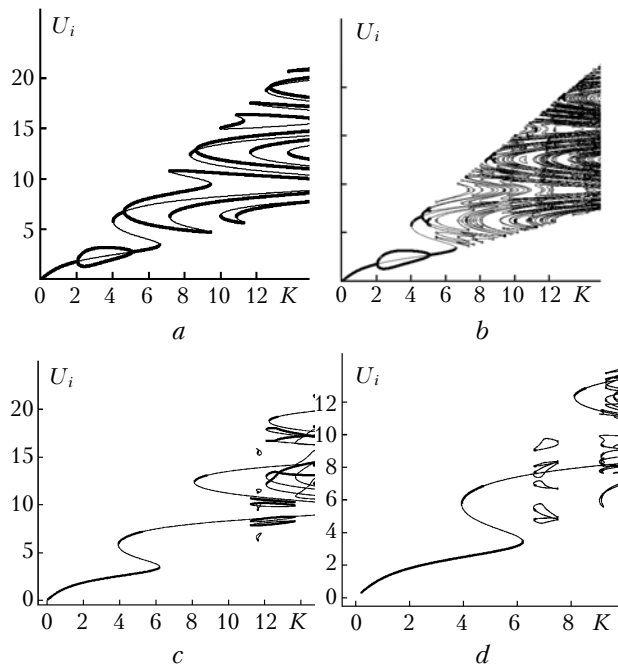


**Fig. 3.** Bifurcation diagrams  $U_i(K)$  ( $\gamma = 0.5$ ) for a single feedback loop NRI at field turn angles in the loop:  $\Delta = 180^\circ$  (a);  $90^\circ$  (b); and for a dual feedback loop interferometer at field turn angles in the circuits:  $\Delta_1 = 90^\circ$  and  $\Delta_2 = 180^\circ$  (c);  $\Delta_1 = 120^\circ$  and  $\Delta_2 = 180^\circ$  (d).

For the parametric regions, where the BD branches are stable, one can exactly predict which statistical behavior will appear in the model of DNRI. Otherwise, dynamic modes are inevitable. Let us make a simulation, for investigation reasons, based on the model (2).

### Characteristics of the dynamic mode in the model of DNRI

Numerical experiments have shown that choosing the DNRI-parameters (nonlinearity coefficients  $K$ , transmission coefficients in a FBL  $\gamma_i$ , lag times  $t_{e_i}$  in FBL<sub>1</sub> and FBL<sub>2</sub>, field turn angle  $\Delta_i$  in each of the FBLs) allows one to perform a series of control modifications.

1) Control over mean values of  $U$  and phase shift between oscillations  $U$  at the (transposition) points of the laser beam cross section.

2) Control over the type and ending of the determination process, which has the form of transient phenomenon: from the periodic duty to the quasiperiodic, from periodic to chaotic, from a static to the periodic, from a periodic in-phase (in two transposition points) to the non-phased periodic, at these points, from a chaotic to the periodic one.

For orienting how the model parameters effect toward the dynamic mode, the fractal dimensionality maps  $D_0(t_{e1}, t_{e2})$  were constructed for the attractor in the model (Fig. 4). The map structure analysis allows certain generalizing statement to be formulated.

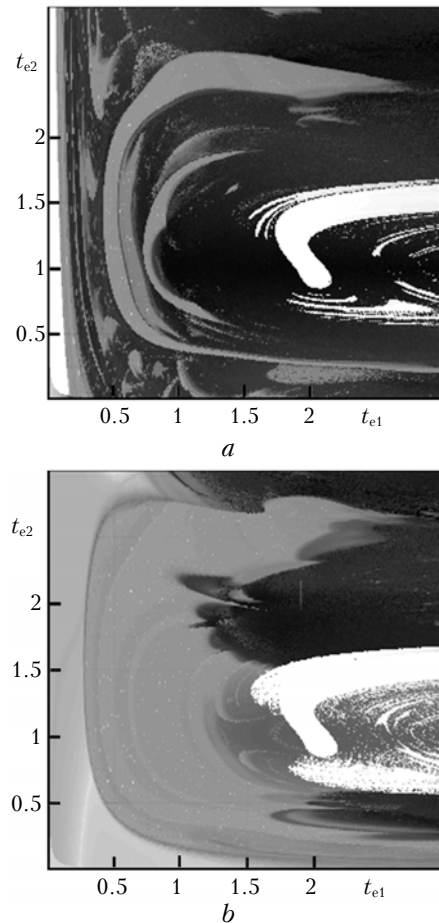


**Fig. 4.** Dependence of the fractal dimensionality  $D_0(t_{e1}, t_{e2})$  on the time-lag ratio in feedback loops. The darker regions correspond to larger values of  $D_0$ ;  $m = 2$ ,  $\Delta_1 = 180^\circ$ ,  $K = 5.5$ ;  $\Delta_2 = 180^\circ$  (a);  $\Delta_2 = 0^\circ$  (b).

If in both FBLs  $\Delta \neq 0$ , a fractal dimensionality of the attractor is not reduced (as a rule, it is essentially increased) in comparison with the case, when  $\Delta_i = 0$ , and the parametric regions, where the fractal dimension of the attractor is high, are extended. These conclusions conform to observations for the behavior of  $U$  at different points of the beam cross section: dynamics of  $U$  becomes complicated as compared with the behavior of  $U$ , when  $\Delta_i = 0$ . According to Ref. 9, large values of fractal dimension  $D_0(t_{e1}, t_{e2})$  are considered as a precondition for high security in the system of confidential communication.

The nature of transient phenomenon in DNRI agrees with the DNRI characteristics demonstrated earlier: complement of NRI by one more FBL enables the formation of either a system of coupled oscillators comprising DNRI, as a whole, or the system of couplings inside one oscillator, such as DNRI.

### Simulation of time-lag hacking by correlation analysis of output field

By use of the  $D_0(t_{e1}, t_{e2})$  maps, one can perform more or less purposeful fitting of the intervals of

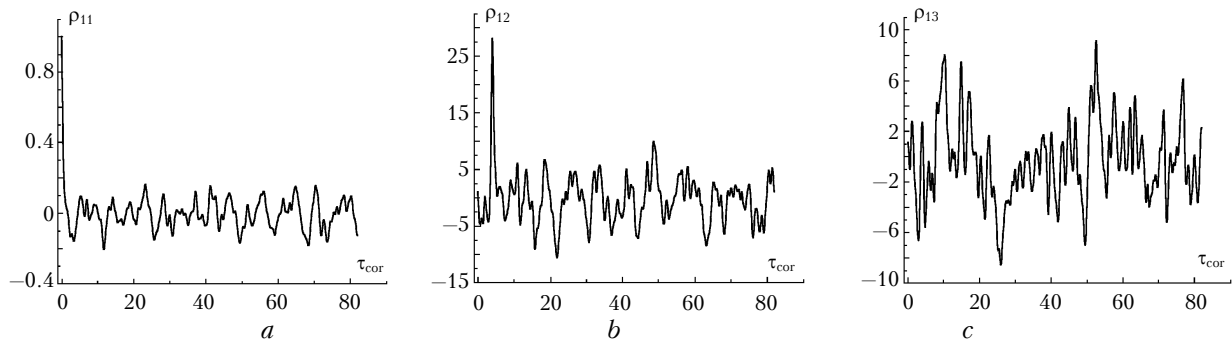


**Fig. 5.** Auto- (*a*) and cross-correlograms (*b*, *c*) for the model of DNRI at  $\Delta_1 = 180^\circ$ ,  $\Delta_2 = 90^\circ$ , lag times in FBL<sub>1</sub> and FBL<sub>2</sub>  $t_{e1}/\tau_n = 1$  and  $t_{e2}/\tau_n = 5$ ,  $\Delta t_e/\tau_n = 4$ , where  $\tau_n = 10^{-9}$  s; losses  $\gamma_1 = \gamma_2 = \sqrt{0.125}$ , nonlinearity coefficient = 10.

physical parameters providing the desirable properties of a DNRI-based encoder. First, this concerns the resistance against hacking the encoder parameters.

The possibility of such a hacking by means of correlation analysis of the optical field amplitudes at some points of the CTP was simulated by use of the model (2). It was established that determination of time lags  $\tau_1$  and  $\tau_2$  in FBL is impossible. However, under certain conditions, calculation of coefficients of autocorrelation  $\rho_{ii}$  or cross-correlation  $\rho_{ij}$  ( $i \neq j$ ) may allow one to reveal their difference  $\tau_1 - \tau_2$ . For instance, for such combinations of the angles, when  $\Delta_1 \neq \Delta_2 \neq 0$  ( $\Delta_1 = 180^\circ$ ,  $\Delta_2 = 90^\circ$  and  $\Delta_1 = 180^\circ$ ,  $\Delta_2 = 120^\circ$ ), dependences of auto- or cross-correlation coefficients are presented in Fig. 5.

As is clear from Fig. 5*b*, the cross-correlation analysis of amplitudes at the points  $i, j$ , that are adjacent in the CTP [in accordance with the numeration ( $j = i + 1$ )], allows revealing the lag time difference  $\Delta t_e = |t_{e2} - t_{e1}|$ . Accuracy of  $\Delta t_e/\tau_n$  is about  $\pm 1.25\%$ . However, if the CTP point search order in the beam cross section is changed, it would become difficult to reveal the value of  $\Delta t_e$  by cross correlation analysis (Fig. 5*c*). In this relation, application of autocorrelation analysis is also inefficient (Fig. 5*a*).

Theoretically, these regularities allow one to identify the CTP, i.e., to determine that points belong to one CTP (dividing points of the beam cross section into the CTP set), and the order of their numeration, but at the expense of long computation time.

Let, for instance, the light field distribution in the beam cross section be presented by an  $m \times N$  matrix, where  $m$  is the number of points in each of the  $N$  isomorphic CTP. Then in the worst circumstances for hacking, revealing of these parameters requires carrying out  $mN(mN - 1) \approx mN^2$  calculations of the cross-correlation coefficients, both  $\rho_{ij}$  and  $\rho_{ji}$ . Nevertheless, even under most favorable conditions ( $m - 1$ ) calculations of the functions  $\rho_{i, i+1}(\tau_{cor})$  are necessary for decoding of only one CTP, and hence, of all the rest. Thus in using the stepper motor with accuracy of angular setting of  $1'$  (for example, a motor produced by Standa company)  $m = 21600$  and in the case of the beam cross section area equal to  $1 \text{ cm}^2$ , the value of  $mN$  can be  $10^4$  as large.

Unlike the model of a single feedback interferometer, the correlation analysis does not allow determining (hacking) the values of the lag times  $t_{e1}$  and  $t_{e2}$  of an optical field in FBL<sub>1</sub> and FBL<sub>2</sub> of a DNRI. Thus, the dual feedback NRI is has higher resistance to hacking its parameters (by means of correlation analysis), rather than a single feedback one.

## Conclusions

The mathematical models of the processes in a dual feedback NRI have been constructed. Formalization of the CTP-structure has been developed, describing the geometrical regularities of transitions from one point to another (shift of light beam in the transverse plane in a DNRI). Diversification of these CTP-structures is revealed depending on combinations of turn angles or on combinations of field shift values in the beam cross section in the FBLs of the DNRI. Two FBLs in the interferometer make it a *multicomponent system* and thus makes up the method to control the laser beam transformation. Manipulating the relations between the FBL-parameters, one can change the scheme of coupling the oscillators forming the DNRI, or configuration of interconnections in the case of a single oscillator.

The simulation data demonstrate that the second feedback loop in a NRI essentially effects the bifurcation of nonlinear phase shifts in a DNRI. It is possible to control the complex dynamics in the model of DNRI (specifically, fractal dimensionality of the attractor) not only by changing the input radiation and nonlinearity parameter as in NRI, but also by choosing combinations for loss / transmission values and field turn angles in FBLs. The model of DNRI has advantages over the single feedback NRI from the point of view of its resistance stability to attempts of hacking the cryptosystem parameters.

All this proves further investigation of the DNRI model aimed at its optimization in developing the deterministic chaos generator as well as its application as an encoder in systems of confidential communication operated in the optical range, including the static operation mode.

### Acknowledgements

The study was supported by Ministry of Education and Science of the Russian Federation (Program: "Development of Scientific Potential of Higher School". Part 3.3) Grant No. 60321 and by the Presidential Grant MK-4701.2006.9.

### References

1. S.A. Akhmanov and M.A. Vorontsov, *J. Opt. Soc. Am. B* **9**, No.1, 78–90 (1992).
2. T. Schwartz, J.W. Fleischer, O. Cohen, H. Buljan, M. Segev, and T. Carmon, *J. Opt. Soc. Am. B* **21**, No. 12, 2197–2205 (2004).
3. S.A. Akhmanov and M.A. Vorontsov, eds., *New Physical Principles of Data-Processing* (Nauka, Moscow, 1990), pp. 263–326.
4. I.V. Izmailov, V.T. Kalayda, A.L. Magazinnikov, and B.N. Poizner, *Izv. Vysh. Ucheb. Zaved., Prikl. Nelin. Dinamika* **7**, No. 5, 47–59 (1999).
5. I.V. Izmailov and B.N. Poizner, in: *Pros. of Intern. Conf. KLIN-2001* (Ulyanovsk, 2001), Vol. 2, pp. 59–61.
6. A.V. Lyachin and B.N. Poizner, *Atmos. Oceanic Opt.* **17**, Nos. 2–3, 126–130 (2004).
7. I.V. Izmailov and B.N. Poizner, *Atmos. Oceanic Opt.* **14**, No. 11, 988–1000 (2001).
8. R. Martin, G.-L. Oppo, G.K. Harkness, A.J. Scroggie, and W.J. Firth, *Opt. Express.* **1**, No. 1, 39–43 (1997).
9. G.D. Van Wiggeren and R. Roy, *Int. J. of Bifurcation and Chaos* **9**, No. 11, 2129–2156 (1999).